

# A speciation study of the aqueous $\text{H}^+/\text{H}_2\text{VO}_4^-/\text{H}_2\text{O}_2/\text{L-}\alpha\text{-alanyl-L-serine}$ system †

András Gorzsás,<sup>a\*</sup> Ingegärd Andersson,<sup>a</sup> Hauke Schmidt,<sup>a</sup> Dieter Rehder<sup>b</sup> and Lage Pettersson<sup>a</sup>

<sup>a</sup> Department of Chemistry, Inorganic Chemistry, Umeå University, SE-901 87 Umeå, Sweden.  
E-mail: Andras.Gorzsas@chem.umu.se; Fax: +46 90 786 9195; Tel: +46 90 786 6325

<sup>b</sup> Institute of Inorganic and Applied Chemistry, University of Hamburg, D-20146 Hamburg, Germany

Received 29th October 2002, Accepted 23rd January 2003

First published as an Advance Article on the web 11th February 2003

A detailed study of the quaternary aqueous  $\text{H}^+/\text{H}_2\text{VO}_4^-/\text{H}_2\text{O}_2/\text{L-}\alpha\text{-alanyl-L-serine}$  (Alaser) system has been performed at 25 °C in 0.150 M Na(Cl) medium, representing the ionic strength of human blood, using quantitative  $^{51}\text{V}$  NMR and potentiometric data (glass electrode). Data were evaluated with the computer program LAKE, which is able to treat combined EMF and NMR data. The  $\text{p}K_{\text{a}}$ -values for Alaser were determined as  $8.04 \pm 0.01$  and  $3.07 \pm 0.01$ . The errors given are  $3\sigma$ . In the ternary  $\text{H}^+/\text{H}_2\text{VO}_4^-/\text{Alaser}$  system, two complexes,  $(\text{H}^+)_p(\text{H}_2\text{VO}_4^-)_q$ - $(\text{Alaser})_r$ , having  $(p, q, r)$  values (0, 1, 1) and (-1, 1, 1) with  $\log \beta_{0,1,1} = 2.42 \pm 0.01$  and  $\log \beta_{-1,1,1} = -5.80 \pm 0.05$  explain all data in the pH region 2.5–9.5. Equilibrium conditions are illustrated in distribution diagrams and structure proposals are given based on  $^1\text{H}$  and  $^{13}\text{C}$  NMR investigations. In the quaternary  $\text{H}^+/\text{H}_2\text{VO}_4^-/\text{H}_2\text{O}_2/\text{Alaser}$  system, six complexes could be found in addition to all binary and ternary complexes over the pH region 2.6–11.1, four with a V/X/Alaser ratio 1 : 1 : 1 and two with a ratio 1 : 2 : 1 (X = peroxo ligand). The formation of the monoperoxo vanadium species is very slow, requiring up to 10 days for complete equilibrium. Significant decomposition of peroxide occurs only in acidic solutions. Chemical shifts, compositions and formation constants for the six quaternary complexes are given, and equilibrium conditions are illustrated in distribution diagrams. The  $\text{H}^+/\text{H}_2\text{VO}_4^-/\text{H}_2\text{O}_2/\text{Alaser}/\text{Alahis}$  system, where Alahis denotes L- $\alpha$ -alanyl-L-histidine, was briefly investigated and no mixed ligand species were detected.

## Introduction

The biochemistry of vanadium and the coordination chemistry of vanadate and several ligands of biochemical interest has been the basis for many interdisciplinary studies during the last two decades.<sup>1,2</sup> Vanadate inhibits many phosphate-metabolising enzymes, which fact also has impact on the insulin-mimetic behaviour<sup>3</sup> of vanadate, peroxovanadate, vanadyl and several vanadium complexes, most probably owing to the inhibition of protein tyrosine phosphatases.<sup>4</sup> In addition to this unspecific, general interaction, vanadium is present in the cofactor of some nitrogenases and haloperoxidases. In nitrogenases, vanadium is an integral part of an iron–sulfur cluster,<sup>5</sup> while in haloperoxidases vanadate(v) is coordinated to the N $^{\epsilon}$  of a histidine. Furthermore, there is a serine at the active site, which has been proposed to participate in the catalytic turnover.<sup>6</sup>

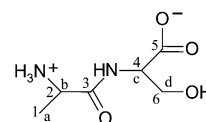
Complexes of vanadate and protein fragments, *i.e.* dipeptides, can be considered as structural models for the unspecific binding of vanadium to proteins. Here, particularly water-soluble complexes are of interest against the background of possible medicinal applications in the field of insulin-mimetics. Accordingly, several  $^{51}\text{V}$  NMR studies have been carried out with different vanadium–dipeptide complexes during the last two decades,<sup>7,8</sup> and recently a comparative study was made to collate ligands with different donor atoms.<sup>9</sup> To address the possible medical use of vanadium complexes, an extensive *in vitro* study had been carried out with promising preliminary results.<sup>10</sup>

In order to obtain information about the coordination of vanadium in biogenic compounds through ligands dominated by nitrogen-functional groups, the vanadium binding to L- $\alpha$ -alanyl-L-histidine (Alahis) has been investigated earlier in 0.600 M Na(Cl) medium<sup>11</sup> and recently reinvestigated in 0.150 M Na(Cl) medium,<sup>12</sup> which represents the ionic strength

of human blood. The revealed coordinating functions here and in all other studied vanadate dipeptide systems are the terminal amino group, the terminal carboxylate and the deprotonated peptide-N.<sup>13–15</sup> This coordination mode is often observed in transition metal dipeptide complexes,<sup>16</sup> and has also been suggested for the  $\text{VO}^{2+}/\text{dipeptide}$  system.<sup>17</sup> Notably, the imidazole residue of Alahis does not coordinate to vanadate.<sup>11</sup> However, if a functional side-chain contains a hydroxy group like in glycylserine, two signals in the  $^{51}\text{V}$  NMR spectra were obtained in contrast to vanadium dipeptide systems with aliphatic or nitrogen containing side-chains. The lower field signal was assigned to an additional coordination of the hydroxy group.<sup>7,8</sup> On the other hand, participation of the hydroxy group of serine in coordination to vanadate was not observed in the crystal structure of  $[\{\text{VO}(\text{van-L-ser})(\text{H}_2\text{O})\}_2(\mu\text{-O})]^{18}$  and  $[\{\text{VO}(\text{sal-D,L-ser})_2(\mu\text{-O})\}^-]$ ,<sup>19</sup> where serine formed a Schiff-base ligand with vanillin or salicylaldehyde.

Peroxide containing vanadate dipeptide systems have been extensively studied by  $^{51}\text{V}$  NMR spectroscopy<sup>20,21</sup> and by X-ray crystallography in the case of the complex with glycyl-glycine,  $(\text{NEt}_4)[\text{VO}(\text{O}_2)(\text{glygly})]$ .<sup>22</sup> For the quaternary  $\text{H}^+/\text{H}_2\text{VO}_4^-/\text{H}_2\text{O}_2/\text{Alahis}$  system, a full speciation has recently been established,<sup>12</sup> and contrary to the solution structures of the ternary  $\text{H}^+/\text{H}_2\text{VO}_4^-/\text{Alahis}$  system, the histidine imidazole was found to be coordinated to vanadium in the presence of peroxo ligand(s).

Against this background, detailed investigations of the ternary  $\text{H}^+/\text{H}_2\text{VO}_4^-/\text{L-}\alpha\text{-alanyl-L-serine}$  (Alaser, Scheme 1)



**Scheme 1** Structure of L- $\alpha$ -alanyl-L-serine (Alaser) including atom labelling for  $^1\text{H}/^{13}\text{C}$  NMR.

**Table 1** Species, notation and formation constants for L- $\alpha$ -alanyl-L-serine (Alaser) [0.150 M Na(Cl), 25 °C]

| $p, q$ | Notation            | $\log \beta(3\sigma)$ | $pK_a$ |
|--------|---------------------|-----------------------|--------|
| -1, 1  | Alaser <sup>-</sup> | -8.04(1)              |        |
| 0, 1   | Alaser              | 0                     | 8.04   |
| 1, 1   | Alaser <sup>+</sup> | 3.07(1)               | 3.07   |

and the quaternary  $H^+/H_2VO_4^-/H_2O_2/Alaser$  systems have been performed in order to reveal the influence of an oxygen containing functional group in the side-chain of the dipeptide in comparison to the corresponding systems with Alahis.<sup>11,12</sup> For equilibrium analyses, quantitative <sup>51</sup>V NMR spectroscopic and potentiometric data have been collected and processed with the computer program LAKE,<sup>23</sup> which is designed to simultaneously treat multimethod data. In addition, the structures of the ternary vanadium complexes with Alaser have been determined using <sup>1</sup>H and <sup>13</sup>C NMR spectroscopy and compared with the structural properties of the corresponding complexes with Alahis.<sup>11</sup>

When different ligands are present simultaneously, the question of mixed ligand complexes arises. In the simplest case, when there are no such complexes formed, the system can be modelled from its subsystems. This was tested in the  $H^+/H_2VO_4^-/H_2O_2/Alaser/Alahis$  system and the results are discussed here.

## Results and discussion

### Subsystems

Equilibrium analyses in the ternary  $H^+/H_2VO_4^-/Alaser$  and the quaternary  $H^+/H_2VO_4^-/H_2O_2/Alaser$  systems necessitate accurate knowledge of the subsystems  $H^+/H_2VO_4^-$ ,  $H^+/Alaser$  and  $H^+/H_2VO_4^-/H_2O_2$  under the same experimental conditions. Speciation and <sup>51</sup>V NMR properties of the hydrolysis of vanadate<sup>24</sup> and the ternary  $H^+/H_2VO_4^-/H_2O_2$  system<sup>25</sup> have already been investigated and published.

For Alaser no acidity constants have been reported so far in 0.150 M Na(Cl) medium. Four potentiometric titrations have been carried out to determine the speciation in this binary system. The acidity constants obtained from these titrations are presented in Table 1, and experimental details are given in the experimental section.

### The $H^+/H_2VO_4^-/Alaser$ system

The full speciation of this ternary system has been established from <sup>51</sup>V NMR data and EMF point solution data, which have been recorded in the pH range 2.5–9.5. The spectra show a rather broad signal at -516 ppm over a wide pH range with an optimum integral intensity near pH 6, and another broad signal at -503 ppm appearing at pH values higher than 7, with a maximum near pH 8.5 (Fig. 1). The program WIN-NMR, distributed by Bruker, was used for the integral evaluation of the spectra, as well as for deconvolution, for instance in the case of the first resonance, which overlaps with one of the decavanadate peaks in acidic solutions. Three series of <sup>51</sup>V NMR spectra have been recorded in order to gain as much information as possible: constant  $c(V)$  with variable  $c(Alaser)$  at neutral pH, constant concentrations of the reactants with variable pH and a constant ratio between vanadate and the ligand ( $V/Alaser = 1/2$ ) with increasing total concentrations. Solutions were stored overnight for equilibration.

The experimental data from 56 spectra were evaluated with the computer program LAKE as described in ref. 11. Different models with different complex compositions have been tested to find the set of complexes that gives the best fit to the data, that is the model with the lowest error squares sum. The result from the LAKE calculations is shown in Table 2.

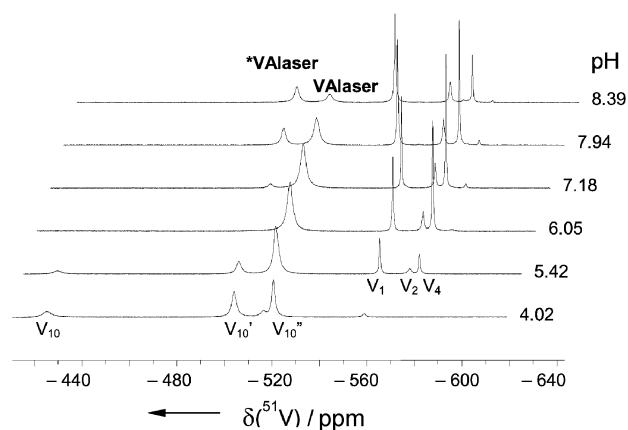


**Fig. 1** <sup>51</sup>V NMR spectra of aqueous solutions containing 4 mM vanadate and 16 mM Alaser at different pH values.

The resonance at -516 ppm can be attributed to a complex,  $(H^+)_p(H_2VO_4^-)_q(Alaser)_s$ , having the  $(p, q, s)$  value (0, 1, 1), VALaser<sup>-</sup>, with  $\log \beta_{0,1,1} = 2.42 \pm 0.01$ . The error given is  $3\sigma$ . No change in the <sup>51</sup>V NMR shift was observed for this compound with varying pH. The signal at -503 ppm was also found without any change in the <sup>51</sup>V NMR shift (Fig. 4), and a complex with a  $(p, q, s)$  value (-1, 1, 1), \*VALaser<sup>2-</sup>, and  $\log \beta_{-1,1,1} = -5.80 \pm 0.05$  gave the best explanation of the experimental data. The different <sup>51</sup>V NMR shifts for the two complexes can suggest different coordination modes of the dipeptide ligand with the possibility of an exchange between these two forms, which is slow on the NMR time scale. Another possibility is that the ligand is coordinated in the same way, *via* the same dentation sites, but the coordination geometry around vanadium is different. Thus, the given  $pK_a$  value (8.22 for VALaser<sup>-</sup>) could be considered as a pseudo  $pK_a$  value.

Fig. 2(a) shows the distribution for all vanadium containing species in the pH range 2–11 at a four-fold excess of Alaser. Under these conditions, the complex VALaser<sup>-</sup> exists from pH 3 to 9.5 and predominates in the pH range 5.5–8. At maximum, 55% of vanadium is integrated into this ternary complex at pH 6. The compound \*VALaser<sup>2-</sup> appears in the pH range 6.5–11 with a maximum amount of 20% at pH 8.5. In the simplified Fig. 2(b), the symbols represent experimental values from <sup>51</sup>V NMR integral data. They fit very well to the calculated curves. A corresponding diagram showing the distribution of the ligand under the same conditions, revealed that about ten percent of the total Alaser is bound to vanadium at maximum.

For comparison, the corresponding distribution diagram with Alahis is shown in Fig. 3 under the same conditions ( $c(V) = 4$  mM,  $c(Alahis) = 16$  mM). Note that the complexation of vanadate with Alaser is almost as strong as with Alahis, the latter binding nearly 70% of total vanadium at maximum (pH ~ 6). With Alaser, however, only anionic and no neutral complexes are formed, as opposed to the presence of the neutral VALahis species in the  $H^+/H_2VO_4^-/Alahis$  system. This is also reflected in the pH regions over which the complexes occur. Since the VALaser species are more negatively charged, they appear towards more alkaline pH, while the VALahis species start to form under more acidic conditions and disappear earlier when going from neutral to alkaline solutions.

<sup>1</sup>H and <sup>13</sup>C NMR measurements have been performed in order to reveal the coordination sites of the dipeptide in the two complexes. Since the oxovanadium(v) unit causes deshielding at the carbon atoms close to the coordinating groups, significant differences in the <sup>13</sup>C shift,  $\Delta\delta = \delta(\text{coordinated ligand}) - \delta(\text{free ligand})$ , indicate complexation. Solutions with maximum amounts of the two complexes (pH ~ 6.5 for VALaser<sup>-</sup> and pH ~ 8.5 for \*VALaser<sup>2-</sup>) and high total concentrations ( $c(V) = 25$  mM,  $c(Alaser) = 100$  mM) were checked by <sup>51</sup>V NMR to

**Table 2** Species, notation, formation constants and  $^{51}\text{V}$  NMR shifts for the  $\text{H}^+/\text{H}_2\text{VO}_4^-/\text{Alaser}$  and  $\text{H}^+/\text{H}_2\text{VO}_4^-/\text{H}_2\text{O}_2/\text{Alaser}$  systems [0.150 M Na(Cl), 25 °C]. Asterisks denote complexes of the same nuclearity, in order of decreasing dominance with increasing number of asterisks

| $p, q, r, s$ | Notation               | $\log\beta(3\sigma)$ | $\text{p}K_a$ | $^{51}\text{V}$ NMR shift/ppm |
|--------------|------------------------|----------------------|---------------|-------------------------------|
| -1, 1, 0, 1  | *VALaser $^{2-}$       | -5.80(5)             |               | -502.6                        |
| 0, 1, 0, 1   | VALaser $^-$           | 2.42(1)              | (8.22)        | -516.5                        |
| -1, 1, 1, 1  | VXAlaser $^{2-}$       | -0.59(8)             |               | -659.2                        |
| 0, 1, 1, 1   | VXAlaser $^-$          | 8.14(3)              | 8.73          | -659.2                        |
| -1, 1, 1, 1  | **VXAlaser $^{2-}$     | -0.72(4)             |               | -676.8                        |
| 0, 1, 1, 1   | *VXAlaser $^-$         | 7.97(3)              | (8.69)        | -655.7                        |
| -1, 1, 2, 1  | VX $_2$ Alaser $^{2-}$ | 5.16(2)              |               | -743.3                        |
| 0, 1, 2, 1   | *VX $_2$ Alaser $^-$   | 11.15(7)             | (5.99)        | -714.0                        |

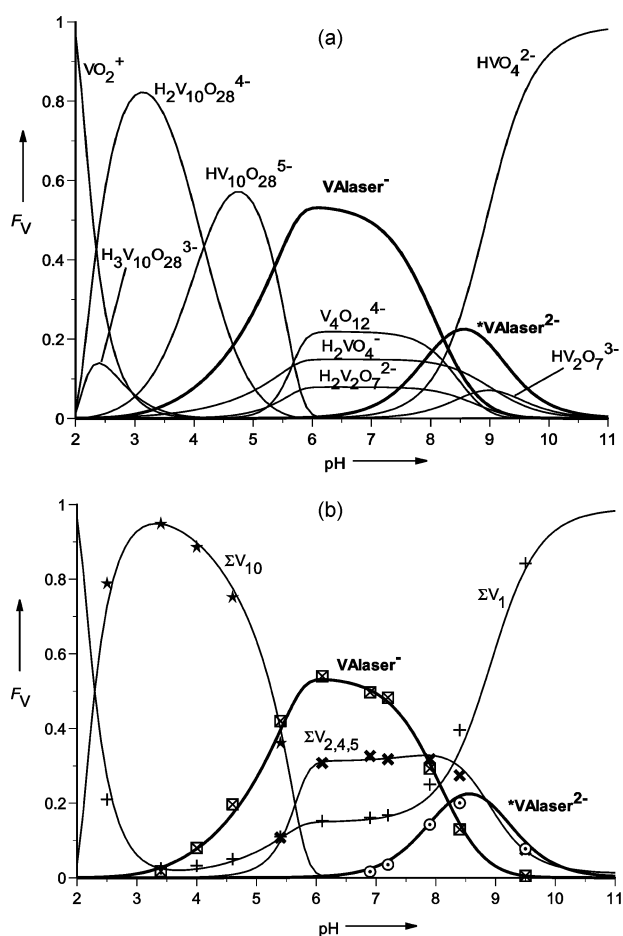


**Fig. 2** Distribution of vanadium,  $F_V$ , vs. pH at  $c(\text{V}) = 4$  mM,  $c(\text{Alaser}) = 16$  mM, in the ternary  $\text{H}^+/\text{H}_2\text{VO}_4^-/\text{Alaser}$  system.  $F_V$  is defined as the ratio between  $c(\text{V})$  in a species and total  $c(\text{V})$ . (a, top) All vanadium containing species are shown except those with  $<2\%$  of total  $c(\text{V})$ . (b, bottom) The sum of the decavanadates, oligovanadates, monovanadates and VALaser species are shown. The symbols represent experimental NMR data points.

have the calculated compositions and then investigated by  $^1\text{H}$  and  $^{13}\text{C}$  NMR spectroscopy.

In the complex VALaser $^-$ , the carbons of the peptide backbone ( $\text{C}_2$ ,  $\text{C}_3$ ,  $\text{C}_4$  and  $\text{C}_5$ , for numbering see Scheme 1) are shifted towards lower field by values between 4.99 and 10.62 ppm (Table 3). These results suggest a coordination of the dipeptide *via* the amino nitrogen, the peptide oxygen and the carboxylate oxygen. The small shift of the methylene carbon indicates that the hydroxyl group in the side chain of the dipeptide is not coordinated to vanadium (Scheme 2(a)). Participation of a functional side chain has not been observed in the corresponding vanadium complexes with Alahis $^{11}$  and alanyltryptophane $^{26}$  either. The  $^1\text{H}$  NMR spectrum for VALaser $^-$  reveals shift differences between  $-0.38$  and  $0.40$  ppm (Table 3). Here, the protons close to the coordinating amino group ( $\text{H}_a$  and  $\text{H}_b$ ) are shifted to higher field, while  $\text{H}_c$  and even

**Table 3**  $^{13}\text{C}$  and  $^1\text{H}$  NMR shifts in the  $\text{H}^+/\text{H}_2\text{VO}_4^-/\text{Alaser}$  system [ $c(\text{V}) = 25$  mM,  $c(\text{Alaser}) = 100$  mM,  $\text{pH} = 7.33/8.52^*$ ]. The notations with asterisks refer to the atoms in the complex \*VAS $^{2-}$ , while the ones without the asterisk to atoms in VAS $^-$

| Atom number $^a$      | $\delta(\text{Alaser})^b/\text{ppm}$ | $\delta(\text{VALaser})/\text{ppm}$ | $\Delta\delta^c/\text{ppm}$ |
|-----------------------|--------------------------------------|-------------------------------------|-----------------------------|
| $\text{C}_1$          | 18.87                                | 20.64                               | 1.77                        |
| $\text{C}_2$          | 59.63                                | 64.62                               | 4.99                        |
| $\text{C}_3$          | 173.20                               | 183.82                              | 10.62                       |
| $\text{C}_4$          | 64.09                                | 70.15                               | 6.06                        |
| $\text{C}_5$          | 178.11                               | 185.33                              | 7.22                        |
| $\text{C}_6$          | 51.48                                | 56.32                               | 4.84                        |
| * $\text{C}_1$        | 21.77                                | 19.04                               | -2.73                       |
| * $\text{C}_2$        | 59.16                                | 71.84                               | 12.68                       |
| * $\text{C}_3$        | 178.39                               | 182.01                              | 3.62                        |
| * $\text{C}_4$        | 64.24                                | 77.66                               | 13.42                       |
| * $\text{C}_5$        | 180.05                               | 185.15                              | 5.10                        |
| * $\text{C}_6$        | 52.37                                | 56.98                               | 4.61                        |
| $\text{H}_a$ (d)      | 1.63                                 | 1.50                                | -0.13                       |
| $\text{H}_b$ (q)      | 4.18                                 | 3.80                                | -0.38                       |
| $\text{H}_c$ (dd)     | 4.38                                 | 4.78                                | 0.40                        |
| $\text{H}_d$ (two dd) | 3.91/3.97                            | 4.03/4.12                           | 0.12/0.15                   |
| * $\text{H}_a$ (d)    | 1.63                                 | 1.71                                | 0.08                        |
| * $\text{H}_b$ (q)    | 3.91                                 | $^d$                                | $^d$                        |
| * $\text{H}_c$ (dd)   | 4.61                                 | $^d$                                | $^d$                        |
| * $\text{H}_d$ (m)    | 4.19                                 | 4.89                                | 0.70                        |

$^a$  See Schemes 1 and 2.  $^b$  Free ligand in the presence of VALaser species.  $^c$   $\Delta\delta = \delta(\text{VALaser}) - \delta(\text{Alaser})$ .  $^d$  Not observed.

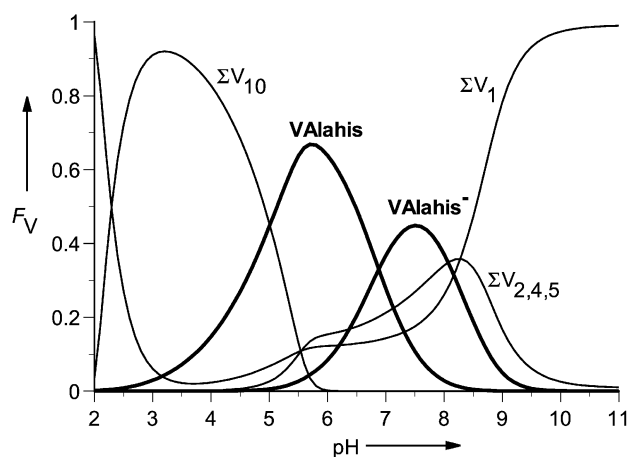
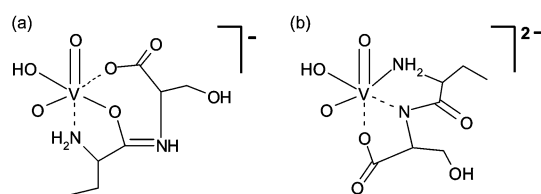


**Fig. 3** Distribution of vanadium,  $F_V$ , vs. pH at  $c(\text{V}) = 4$  mM,  $c(\text{Alahis}) = 16$  mM, in the ternary  $\text{H}^+/\text{H}_2\text{VO}_4^-/\text{Alahis}$  system, where Alahis represents L- $\alpha$ -alanyl-L-histidine. For clarity, the sum of the decavanadates, oligovanadates and monovanadates are shown.

$\text{H}_d$  are shifted downfield. This is perhaps owing to the relatively weak interaction between vanadate and the amino group in comparison to the other coordinating functional groups, especially the peptide oxygen.

In the complex \*VALaser $^{2-}$ , the resonance for \* $\text{C}_2$  shows a larger shift towards lower field compared to the one in VALaser $^-$ . The reason could be a stronger coordination of



Scheme 2 Proposed structures of (a) VALaser<sup>-</sup> and (b) \*VALaser<sup>2-</sup>.

the ligand in the case of \*VALaser<sup>2-</sup> as compared to that of VALaser<sup>-</sup>. The difference of the shift for the methylene carbon \*C<sub>6</sub> in \*VALaser<sup>2-</sup> is almost the same as in VALaser<sup>-</sup>, which indicates that the hydroxy group is not coordinated in this case either. Deprotonation of this function is unlikely, owing to this result and potentiometric data. Apart from this similarity, the coordination mode of the dipeptide in \*VALaser<sup>2-</sup> seems to be different from that of in VALaser<sup>-</sup>. From the <sup>13</sup>C chemical shift data (Table 3), the dipeptide seems to be tridentate in \*VALaser<sup>2-</sup> as well, but most probably using different dentation sites than in VALaser<sup>-</sup>: the amide nitrogen, carboxylate oxygen, and the deprotonated peptide nitrogen instead of the peptide oxygen (Scheme 2(b)). This explains the difference between the <sup>51</sup>V chemical shifts of the two complexes and locates the peptide nitrogen as the source of deprotonation. The formation of two five-membered ring is favourable and the same dentation sites were observed earlier for the ternary complexes of vanadate with other dipeptides, such as Alahis,<sup>11</sup> prolylalanine and alanyl glycine.<sup>15</sup>

#### The H<sup>+</sup>/H<sub>2</sub>VO<sub>4</sub><sup>-</sup>/H<sub>2</sub>O<sub>2</sub>/Alaser system

In this system five new resonances for quaternary complexes appear in addition to those of the ternary peroxovanadium species over the wide pH range 3–10. By comparison with the recently investigated H<sup>+</sup>/H<sub>2</sub>VO<sub>4</sub><sup>-</sup>/H<sub>2</sub>O<sub>2</sub>/Alahis system,<sup>12</sup> and by means of LAKE calculations the signals can be assigned to VXAlaser<sup>2-</sup>/VXAlaser<sup>-</sup> (–659 ppm), \*VXAlaser<sup>-</sup> (–656 ppm), \*\*VXAlaser<sup>2-</sup> (–677 ppm), VX<sub>2</sub>Alaser<sup>2-</sup> (–743 ppm) and \*VX<sub>2</sub>Alaser<sup>-</sup> (–714 ppm), where X is used instead of the peroxo ligand to shorten the formulae (Fig. 4). The species VXAlaser<sup>2-</sup>/VXAlaser<sup>-</sup>, \*VXAlaser<sup>-</sup>, \*\*VXAlaser<sup>2-</sup> and VX<sub>2</sub>Alaser<sup>2-</sup>, \*VX<sub>2</sub>Alaser<sup>-</sup> when having the same nuclearity, are differentiated by the asterisks, in the way that the more asterisks in the notation, the least dominating the species is. No changes in the chemical shifts with pH occur for any of the five resonances (Fig. 4). Calculations showed, however, that the species VXAlaser<sup>2-</sup> undergoes protonation, even though its chemical shift remains unchanged. It indicates that the protonation occurs remotely, not affecting the electronic environment of vanadium. No protonation/deprotonation was observed for any of the other quaternary species.

It is worth mentioning that all quaternary species can be deduced from ternary VALaser species with addition of one or two peroxides. Similarly to other systems,<sup>9</sup> spectra can be divided into two regions, the low field part corresponding to species containing VX moieties, and the high field part for complexes with VX<sub>2</sub> moieties. In addition to this feature of the chemical shift curve, it also provides information about the pH range over which a certain species exists (Fig. 4).

Equilibria in this quaternary system show somewhat similar properties to that of the corresponding system with Alahis.<sup>12</sup> They are slow owing to slow formation of the monoperoxovanadate dipeptide complexes and slow decomposition of decavanadates initially formed in acidic solutions. However, if the dipeptide is added to equilibrated peroxovanadate solutions with a *c*(H<sub>2</sub>O<sub>2</sub>) to *c*(V) ratio less than two, the formation of ternary VALaser complexes is faster than the formation of quaternary monoperoxo vanadate species. Thus, decomposition of these ternary complexes here has to be taken into account as well. Serial <sup>51</sup>V NMR measurements were carried

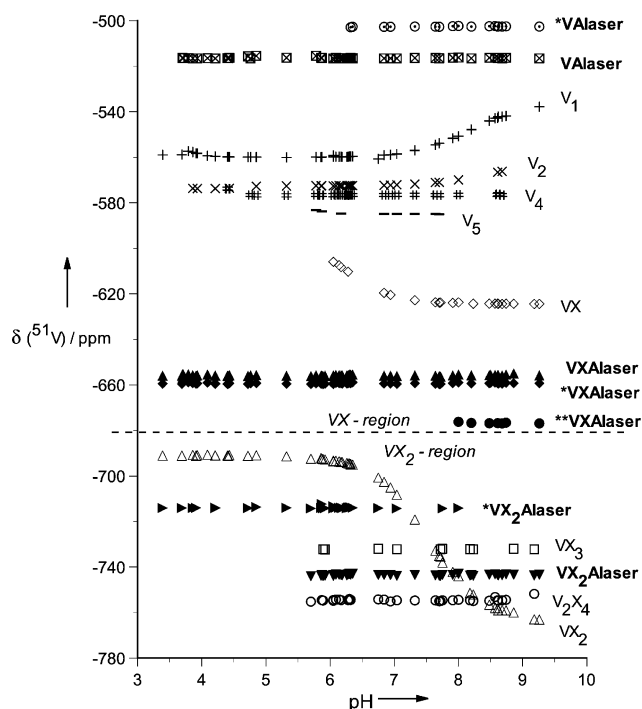
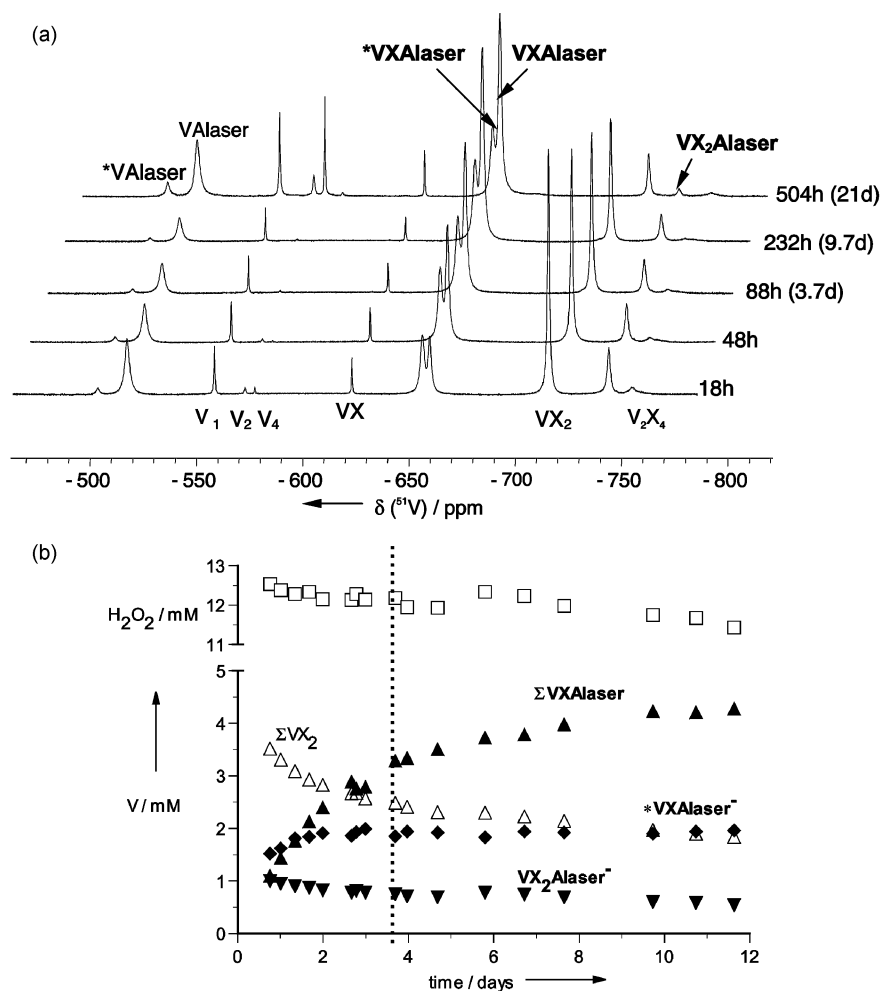


Fig. 4 <sup>51</sup>V NMR chemical shift values for the species present in the quaternary H<sup>+</sup>/H<sub>2</sub>VO<sub>4</sub><sup>-</sup>/H<sub>2</sub>O<sub>2</sub>/Alaser system vs. pH, except for decavanadates.

out after adding hydrogen peroxide or the dipeptide as the last component to determine the equilibration time and the influence of decavanadates and peroxide decomposition. A total of 11 serial measurements were recorded with different *c*(V)/*c*(H<sub>2</sub>O<sub>2</sub>)/*c*(Alaser) ratios in the pH range 3.7–8.2. When solutions are prepared in the way that the dipeptide is added to equilibrated peroxovanadate solutions with *c*(H<sub>2</sub>O<sub>2</sub>)/*c*(V) ratios higher than two, the formation of the bisperoxo complexes (VX<sub>2</sub>Alaser<sup>2-</sup> and \*VX<sub>2</sub>Alaser<sup>-</sup>) is already accomplished after 2 h, while at lower ratios the formation of the quaternary monoperoxo species takes up to about 10 days (Fig. 5(a) and (b)).

In weakly to more acidic solutions VX<sub>2</sub>Alaser<sup>2-</sup> does not appear, but the minor \*VX<sub>2</sub>Alaser<sup>-</sup> complex exists even at as low pH values as 3. Contrary to the comparatively fast equilibration in the case of the bisperoxo species, the formation of the monoperoxo vanadium complexes is very slow. Fig. 5(a) shows the results of a serial <sup>51</sup>V NMR measurement at pH 7.5. The equilibration time was set to 88 h (dashed line in Fig. 5(b)) in the calculations and all solutions for quantitative measurements were allowed to equilibrate for that time after addition of hydrogen peroxide. Although the VXAlaser species did not reach complete equilibrium over this time, it does not affect the results substantially. This was clearly confirmed when further calculations were made on data older than 9 days (last three points in Fig. 5(b)) and the resulting formation constant was in good agreement with that obtained after 88 h (log β = 8.31 and 8.14, respectively). Owing to significant decomposition of peroxide in acidic solutions, only <sup>51</sup>V NMR integral data in the range pH 5–10 were used for the LAKE calculations. In this region, the peroxide content of the solutions was found to be exceptionally stable, no substantial peroxide loss was observed even after 12 days (Fig. 5(b), upper part).

The complexation of vanadium with peroxide is quite strong; at a ratio H<sub>2</sub>O<sub>2</sub>/V = 2, most of the vanadium is present in the form of inorganic diperoxovanadates and, at pH values higher than 7, in the quaternary complex VX<sub>2</sub>Alaser<sup>2-</sup>. To get appreciable amounts of quaternary monoperoxospecies, a lower H<sub>2</sub>O<sub>2</sub>/V ratio and excess of the dipeptide are necessary. The former is needed to hinder the formation of VX<sub>2</sub>Alaser<sup>2-</sup>, while the latter is required to suppress the strong VX<sub>2</sub> species.



**Fig. 5** (a, top)  $^{51}\text{V}$  NMR spectra of an aqueous solution containing 10 mM vanadate, 13 mM hydrogen peroxide and 40 mM Alaser at pH 7.5 after different reaction times. (b, bottom) Concentrations of the main complexes and  $\text{H}_2\text{O}_2$  vs. time in the aforementioned solution.

The  $^{51}\text{V}$  NMR integral data for the signals of all quaternary species ( $-656$ ,  $-659$ ,  $-677$ ,  $-714$  and  $-743$  ppm) were evaluated with the computer program LAKE to find compositions and formation constants for the set of complexes which explain the experimental data best. The results of these calculations are presented in Table 2 and the speciation is in accordance with the preliminary assignments. The low  $3\sigma$  values obtained even in the case of minor species illustrate the power of combined NMR and potentiometric techniques in speciation studies of complicated systems.

For the signal at  $-743$  ppm, a quaternary diperoxo complex,  $\text{VX}_2\text{Alaser}^{2-}$ , gives the best fit to the data. The complex exists in the pH range 6–9, and no change in its chemical shift was observed owing to protonation/deprotonation. There is, however, a minor protonated species with the same nuclearity ( $^*\text{VX}_2\text{Alaser}^-$ ) being present from pH about 3.5–8 with a constant chemical shift of  $-714$  ppm. The two signals for the quaternary monoperoxo complexes  $\text{VXAlaser}^{2-}/\text{VXAlaser}^-$  and  $^*\text{VXAlaser}^-$  at  $-659$  and  $-656$  ppm, respectively, exist over an even wider pH range (3–10) with maximum amounts at pH 6, while the one for  $^{**}\text{VXAlaser}^{2-}$  at  $-677$  ppm is present only at pH values between 7.5 and 9.5, with a maximum at about pH 8.5. All these four species have the same nuclearity but only one of them shows a protonation step. This protonation/deprotonation, however, is not accompanied with any change in the  $^{51}\text{V}$  NMR shift, indicating that the proton transfer occurs remotely from vanadium, not disturbing its electronic environment.

Figs. 6 and 7 show the distribution of vanadium,  $F_V$ , as a function of pH at different conditions. At a  $\text{H}_2\text{O}_2/\text{V}$  ratio 2.2

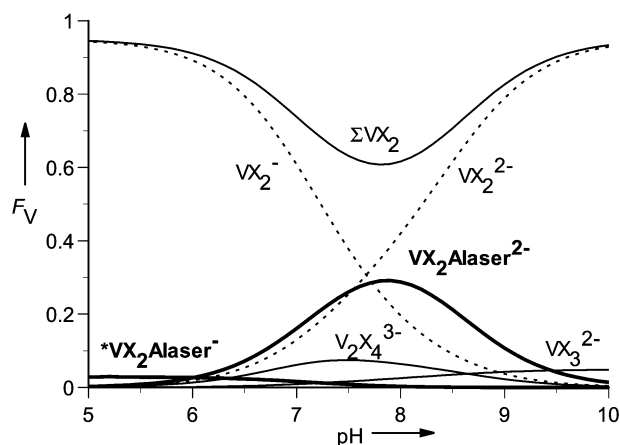


**Fig. 6** Distribution of vanadium,  $F_V$ , vs. pH in the quaternary  $\text{H}^+/\text{H}_2\text{VO}_4^-/\text{H}_2\text{O}_2/\text{Alaser}$  system at  $c(\text{V}) = 10$  mM,  $c(\text{H}_2\text{O}_2) = 22$  mM,  $c(\text{Alaser}) = 40$  mM.

( $c(\text{V}) = 10$  mM,  $c(\text{H}_2\text{O}_2) = 22$  mM,  $c(\text{Alaser}) = 40$  mM, Fig. 6), no monoperoxo vanadium species are formed. However, not more than 30% of vanadium is present in  $\text{VX}_2\text{Alaser}^{2-}$  ( $-743$  ppm) at its optimum at pH 8. Ternary inorganic peroxovanadates, in particular  $\text{VX}_2^-$  and  $\text{VX}_2^{2-}$ , are the predominating species over the whole range. Thus, the quaternary complex  $\text{VX}_2\text{Alaser}^{2-}$  is not nearly as strong as the corresponding complex in the recently investigated system with Alahis.<sup>12</sup>

At a lower  $\text{H}_2\text{O}_2/\text{V}$  ratio (1.3,  $c(\text{V}) = 10$  mM,  $c(\text{H}_2\text{O}_2) = 13$  mM,  $c(\text{Alaser}) = 40$  mM, Fig. 7) monoperoxo species appear,

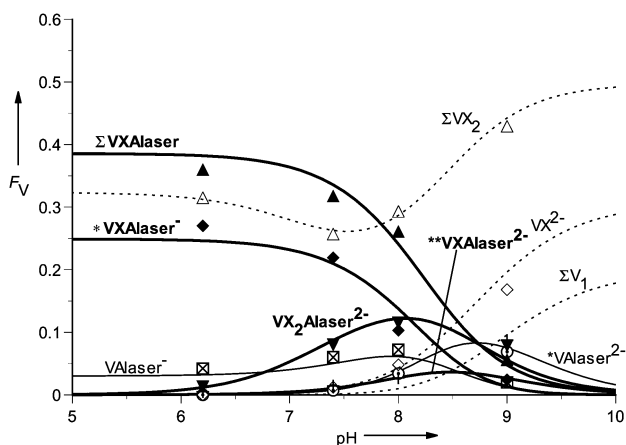


Fig. 7 Distribution of vanadium,  $F_V$ , vs. pH in the quaternary  $H^+/H_2VO_4^-/H_2O_2/Alaser$  system at  $c(V) = 10$  mM,  $c(H_2O_2) = 13$  mM,  $c(Alaser) = 40$  mM. Symbols represent experimental points.

binding more than 60% of vanadium at pH values between 5 and 7. With this ratio, however, ternary  $VAlaser^-$  species are also present. At the physiological pH of 7.4, the quaternary bisperoxo vanadium complex  $VX_2Alaser^{2-}$  integrates about 10% of the total vanadium, and in more alkaline solutions (pH above 8) the inorganic diperoxovanadate species start to dominate. Symbols in this figure represent experimental points, and the fit to the calculated curves is very good, considering the slow equilibria and relatively broad, overlapping peaks of the different  $VXAlaser$  species.

Comparison with the recently investigated quaternary  $H^+/H_2VO_4^-/H_2O_2/Alahis$  system<sup>12</sup> reveals that peroxovanadate and diperoxovanadate form only weak complexes with Alaser, while the complex of diperoxovanadate and Alahis, where the imidazole residue coordinates to the vanadium, is quite strong. Thus, complexation of vanadate with oxygen containing functional groups seems not to be favoured in the presence of peroxide compared to that of with aromatic nitrogen containing ligands<sup>9</sup> (Alahis<sup>12</sup> or imidazole itself<sup>25</sup>). Furthermore, only anionic and no neutral complexes are formed with Alaser, like in the corresponding ternary system.

Modelling was carried out to elucidate the behaviour of different peroxovanadate/ligand complexes under hypothetical physiological conditions.<sup>9</sup> Since the biological studies showed that vanadium complexes mimic insulin efficiently at 1  $\mu$ M concentration,<sup>10</sup> the vanadate total concentration was set to this value. A tenfold excess of hydrogen peroxide and a 20,000 fold excess of the ligands were applied in the modelling. With Alahis, approximately ninety percent of vanadium was bound in quaternary diperoxovanadate–Alahis complexes at pH = 7.4, and less than ten percent of the total vanadium was found in ternary diperoxovanadates. With Alaser, however, these inorganic diperoxovanadates contribute to approximately thirty percent, and quaternary  $VX_2Alaser$  species to only about ten percent at the same pH. The dominating species are the monoperoxovanadate–Alaser complexes, having approximately fifty percent of total vanadium bound. The remaining ten percent was found in the ternary  $VAlaser^-$  species. It clearly shows the difference between the complexing behaviour of the two dipeptides in peroxovanadates, and illustrates the preference of diperoxovanadates towards aromatic nitrogen donor atoms.

The determination of the structures of the formed peroxovanadate complexes in solution can prove to be a difficult task and is beyond the scope of the present study. Proposals, however, can be given, based on already known structures of similar peroxovanadium compounds and on the tentative structures of the ternary complexes  $VAlaser^-$  and  $*VAlaser^{2-}$  (Scheme 2(a) and (b)). We can safely assume that in all of the monoperoxovanadate–Alaser complexes, the peroxy ligand is bound to vanadium in a side-on manner, extending the

coordination number of the central metal from 6 to 7, changing the geometry from octahedral to pentagonal bipyramidal. This does not require alteration of coordination mode for the dipeptide to produce more than one possible isomer. Considering that there is difference already between  $VAlaser^-$  and  $*VAlaser^{2-}$ , adding a peroxy ligand to each would produce different monoperoxovanadate complexes, in accordance to our observations. In the case of diperoxovanadate complexes ( $VX_2Alaser^{2-}$  and  $*VX_2Alaser^-$ ) it requires further investigations to determine whether the ligand is still tridentate or not. Problems arise, however, with multinuclear NMR, as the stability of the compounds, their maximum possible concentration and relative purity from each other are factors to be controlled simultaneously. Crystallography could give further insight, but our efforts to obtain appropriate crystals have been unsuccessful so far.

### The $H^+/H_2VO_4^-/H_2O_2/Alaser/Alahis$ system

In case there are different ligands present, mixed ligand complexes can in theory form. This is of particular interest in understanding the fate of vanadium (complexes) in the bloodstream, where many different ligands are present in high excess to vanadium. This was clearly illustrated when mixed ligand species were observed in the case of vanadium(IV) complexes of picolinic acid or 6-methylpicolinic acid and low molecular mass blood serum ligands such as oxalate, lactate, citrate and phosphate.<sup>27</sup>

On the other hand, if no formation of mixed ligand complexes occurs, the system can be modelled from its subsystems. This has been tested for peroxovanadates with the ligands Alahis and Alaser. Since none of these ligands forms species where there is more than one ligand present, no mixed ligand complex was expected when having both ligands present simultaneously. A  $^{51}V$  NMR spectrum was recorded from a  $c(V) = 10$  mM solution containing a small excess of hydrogen peroxide ( $c(H_2O_2) = 22$  mM) and the two ligands. Since Alaser is a much weaker complexation agent than Alahis, the former was in excess ( $c(Alaser) = 40$  mM,  $c(Alahis) = 8$  mM). As expected, no other resonances than those already known from the two quaternary systems were detected, indicating that no mixed-ligand species were formed. To make sure that a resonance from a mixed ligand species is not in perfect overlap with any of the known resonances, the spectrum was evaluated and the experimental points fitted perfectly to the calculated distribution curves.<sup>9</sup> This proves that no mixed-ligand Alahis–Alaser species are formed at the prevailing pH value (6.7) and illustrates how well the model from the subsystems can describe speciation even with different ligands present.

Another result from this experiment was that the bisperoxo complexes with Alahis still predominate over the corresponding Alaser species, despite the five-fold excess of the latter ligand. It again emphasizes the preference of peroxovanadium species towards aromatic nitrogen donor ligands, over aliphatic nitrogen or oxygen donating ligands.<sup>9</sup>

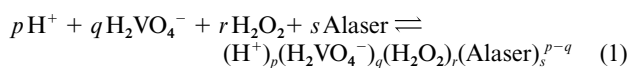
## Experimental

### Chemicals and analyses

L- $\alpha$ -Alanyl-L-serine,  $C_6H_{12}N_2O_4$  (Bachem), had been stored below 0  $^{\circ}C$ , and was tempered to 25  $^{\circ}C$  prior to use. Possible interactions between Alaser and hydrogen peroxide have been checked by  $^1H$  and  $^{13}C$  NMR measurements which show no changes after addition of  $H_2O_2$ . All the other chemicals were used as described in ref. 12.

### Notation

The equilibria studied are written with the components  $H^+$ ,  $H_2VO_4^-$ ,  $H_2O_2$  and Alaser. Thus, complexes are formed according to the following equation



Formation constants are denoted  $\beta_{p,q,r,s}$  and complexes are given the notation  $(p,q,r,s)$  or  $V_qX_r\text{Alaser}_s^{p-q}$ . X is used instead of the peroxy ligand to shorten the formulae. The total concentrations of vanadate, hydrogen peroxide and L- $\alpha$ -alanyl-L-serine are denoted  $c(\text{V})$ ,  $c(\text{H}_2\text{O}_2)$  and  $c(\text{Alaser})$ , respectively, and are given in mM in the figures.

### Equilibration of the solutions

In the ternary  $\text{H}^+/\text{H}_2\text{VO}_4^-/\text{Alaser}$  system, the solutions were stored overnight before the measurements for equilibration. In the quaternary  $\text{H}^+/\text{H}_2\text{VO}_4^-/\text{H}_2\text{O}_2/\text{Alaser}$  system, the samples were in general prepared by adding hydrogen peroxide to the equilibrated solutions containing vanadate and dipeptide. However, cross-checks were performed by adding the dipeptide or the acid/base at the end. The process of complex formation is slowed down by the decomposition of the initially formed decavanadates in the pH range 3–6, which takes approximately 16 h. The formation of the monoperoxy species, however, is an even slower process, requiring nearly 10 days for complete equilibration of the  $\text{VXAlaser}$  species. Calculations showed that an equilibrium time of 88 h provides reasonably good formation constants; therefore, the solutions were allowed to stand for this time before measurements. Owing to substantial decomposition of peroxide in acidic solutions, only  $^{51}\text{V}$  NMR integral data in pH 5–10 were used for calculations. Although the decomposition of peroxide is only marginal in this pH range, it was taken into account.

### Potentiometric measurements

The EMF measurements in the binary  $\text{H}^+/\text{Alaser}$  system were carried out as potentiometric titrations in 0.150 M NaCl medium at 25 °C with an automated potentiometric titrator as described in ref. 11. For the ternary  $\text{H}^+/\text{H}_2\text{VO}_4^-/\text{Alaser}$  and quaternary  $\text{H}^+/\text{H}_2\text{VO}_4^-/\text{H}_2\text{O}_2/\text{Alaser}$  systems, pH was measured as described in ref. 12.

### NMR measurements

Spectra were recorded on a Bruker AMX-500 MHz spectrometer as described in refs. 12 and 25.  $^{51}\text{V}$  NMR and  $^1\text{H}/^{13}\text{C}$  NMR chemical shifts are given in ppm relative to  $\text{VOCl}_3$  and TMS, respectively.

### Potentiometric data

The acidity constants for Alaser were determined from four titrations with a total of 88 points. The pH range was 1.9–10.6 and the total concentration range  $5 < c(\text{Alaser})/\text{mM} < 20$ . Owing to slow equilibria in the ternary  $\text{H}^+/\text{H}_2\text{VO}_4^-/\text{Alaser}$  and quaternary  $\text{H}^+/\text{H}_2\text{VO}_4^-/\text{H}_2\text{O}_2/\text{Alaser}$  systems and to the decomposition of hydrogen peroxide, particularly in acidic solutions, no titrations were performed in these systems. Potentiometric data for these systems were obtained by measurement of 'point' solutions with a combination electrode.

### NMR data

In the ternary  $\text{H}^+/\text{H}_2\text{VO}_4^-/\text{Alaser}$  system 56 spectra were recorded in the ranges  $2.5 < \text{pH} < 9.5$ ,  $4 < c(\text{V})/\text{mM} < 16$  and  $2 < c(\text{Alaser})/\text{mM} < 32$ . In the quaternary  $\text{H}^+/\text{H}_2\text{VO}_4^-/\text{H}_2\text{O}_2/\text{Alaser}$  system a total of 78 spectra and 11 serial measurements were recorded in the ranges  $2.64 < \text{pH} < 11.1$ ,  $2.8 < c(\text{V})/\text{mM} < 40$ ,  $2.5 < c(\text{H}_2\text{O}_2)/\text{mM} < 52.2$  and  $12.1 < c(\text{Alaser})/\text{mM} < 85$ . The pH of each solution was measured directly after recording the NMR spectrum. In the calculations, altogether 35 spectra were used, owing to limitations in pH and required equilibrium time.

### Calculations

The EMF and quantitative  $^{51}\text{V}$  NMR data were evaluated using the least squares program LAKE<sup>23</sup> as described in ref. 11. The LAKE program is able to calculate formation constants from a combination of different kinds of data. In the present work, potentiometric and quantitative  $^{51}\text{V}$  NMR integral data have been used. Calculation and plotting of distribution diagrams were performed using WINSGW,<sup>28</sup> a program package based on the SOLGASWATER algorithm.<sup>29</sup>

### Acknowledgements

This work was supported by the Swedish Natural Science Research Council and the European Union (COST project D21/0009–05).

### References

- 1 D. Rehder, *Angew. Chem.*, 1991, **103**, 152; D. Rehder, *Angew. Chem., Int. Ed. Engl.*, 1991, **30**, 148; D. Rehder, *Coord. Chem. Rev.*, 1999, **182**, 297; A. Butler and C. J. Carrano, *Coord. Chem. Rev.*, 1991, **109**, 61; R. Wever and K. Kustin, *Adv. Inorg. Chem.*, 1990, **35**, 81.
- 2 *Vanadium Compounds: Chemistry, Biochemistry and Therapeutic Applications*, ACS Symposium Series 711, ed. A. S. Tracey and D. C. Crans, ACS Publications, Washington, 1998.
- 3 K. H. Thompson, J. H. McNeill and C. Orvig, *Chem. Rev.*, 1999, **99**, 2561.
- 4 I. Goldwasser, D. Gefel, E. Gershonov, M. Fridkin and Y. Shechter, *J. Inorg. Biochem.*, 2000, **80**, 21.
- 5 J. Chen, J. Christiansen, R. C. Tittsworth, B. J. Hales, S. J. George, D. Coucouvanis and S. P. Cramer, *J. Am. Chem. Soc.*, 1993, **115**, 5509.
- 6 A. Messerschmidt and R. Wever, *Proc. Natl. Acad. Sci. USA*, 1996, **93**, 392; A. Messerschmidt, L. Prade and R. Wever, *Biol. Chem.*, 1997, **378**, 309; M. Weyand, H.-J. Hecht, M. Kieß, M.-F. Liaud, H. Vilter and D. Schomburg, *J. Mol. Biol.*, 1999, **293**, 595.
- 7 D. Rehder, *Inorg. Chem.*, 1988, **27**, 4312.
- 8 J. S. Jaswal and A. S. Tracey, *Can. J. Chem.*, 1991, **69**, 1600.
- 9 Part 8: L. Pettersson, I. Andersson and A. Gorzšás, *Coord. Chem. Rev.*, in press.
- 10 D. Rehder, J. Costa Pessoa, C. F. G. C. Geraldes, M. M. C. A. Castro, T. Kabanos, T. Kiss, B. Meier, G. Micera, L. Pettersson, M. Rangel, A. Salifoglou, I. Turel and D. Wang, *J. Biol. Inorg. Chem.*, 2002, **7**, 384.
- 11 K. Elvingsson, M. Fritzsche, D. Rehder and L. Pettersson, *Acta Chem. Scand.*, 1994, **48**, 878.
- 12 H. Schmidt, I. Andersson, D. Rehder and L. Pettersson, *Chem. Eur. J.*, 2001, **7**, 251.
- 13 M. Fritzsche, V. Vergopoulos and D. Rehder, *Inorg. Chim. Acta*, 1993, **211**, 11.
- 14 D. C. Crans, H. Holst, A. D. Keramidas and D. Rehder, *Inorg. Chem.*, 1995, **34**, 2524.
- 15 M. Fritzsche, K. Elvingsson, D. Rehder and L. Pettersson, *Acta Chem. Scand.*, 1997, **51**, 483.
- 16 I. Sóvágó, *Biocoordination Chemistry*, ed. K. Burger, Ellis Horwood, New York, 1990, ch. 4.
- 17 J. Costa Pessoa, S. M. Luz and R. D. Gillard, *J. Chem. Soc., Dalton Trans.*, 1997, 569.
- 18 C. Grüning, H. Schmidt and D. Rehder, *Inorg. Chem. Commun.*, 1999, **2**, 57.
- 19 J. Costa Pessoa, J. A. L. Silva, A. L. Vieira, L. Vilas-Boas, P. O'Brien and P. Thornton, *J. Chem. Soc., Dalton Trans.*, 1992, 1745.
- 20 A. S. Tracey and J. S. Jaswal, *J. Am. Chem. Soc.*, 1992, **114**, 3835.
- 21 A. S. Tracey and J. S. Jaswal, *Inorg. Chem.*, 1993, **32**, 4235.
- 22 F. W. B. Einstein, R. J. Batchelor, S. J. Angus-Dunne and A. S. Tracey, *Inorg. Chem.*, 1996, **35**, 1680.
- 23 N. Ingri, I. Andersson, L. Pettersson, A. Yagasaki, L. Andersson and K. Holmström, *Acta Chem. Scand.*, 1996, **50**, 717.
- 24 K. Elvingsson, A. González-Baró and L. Pettersson, *Inorg. Chem.*, 1996, **35**, 3388.
- 25 I. Andersson, S. Angus-Dunne, O. W. Howarth and L. Pettersson, *J. Inorg. Biochem.*, 2000, **80**, 51.
- 26 M. Fritzsche, Ph. D. Thesis, University of Hamburg, Germany, 1995, p. 47.
- 27 E. Kiss, E. Garribba, G. Micera, T. Kiss and H. Sakurai, *J. Inorg. Biochem.*, 2000, **78**, 97.
- 28 M. Karlsson and J. Lindgren, personal communication.
- 29 G. Eriksson, *Anal. Chim. Acta.*, 1970, **112**, 375.